Cause-and-effect in Mediterranean erosion

Roberts, Neil; Allcock, Samantha L.; Barnett, Hannah; Mather, Anne; Eastwood, Warren; Jones, Matthew; Primmer, Nick; Yiğitbaşıoğlu, Hakan; Vannière, Boris

DOI:
10.1016/j.geomorph.2018.11.016

Cause-and-effect in Mediterranean erosion: The role of humans and climate upon Holocene sediment flux into a central Anatolian lake catchment

Neil Roberts[1], Samantha L. Allcock[2], Hannah Barnett[1], Anne Mather[1], Warren J. Eastwood[3], Matthew Jones[4], Nick Primmer[4], Hakan Yiğitbaşıoğlu[5] and Boris Vannière[6]

[1] School of Geography, Earth and Environmental Sciences, University of Plymouth, Drake Circus, Plymouth, PL4 8AA, UK

[2] Next Steps South West, University of Plymouth, Drake Circus, Plymouth, PL4 8AA, UK

[3] School of Geography, Earth and Environmental Sciences, University of Birmingham, B15 2TT, UK

[4] School of Geography, University of Nottingham, NG7 2RD, UK

[5] Dil ve Tarih-Coğrafya Fakültesi, Ankara University, Turkey

[6] CNRS, CHRONO-ENVIRONNEMENT UMR 6249, MSHE USR 3124, Université Bourgogne Franche-Comté, F-25000 Besançon, France

Corresponding author: email: cnroberts@plymouth.ac.uk

Abstract

The debate in historical geomorphological studies about the causes of erosion in regions such as the Mediterranean has been long-standing. The relative roles of climate change and human impacts can be difficult to disentangle in the absence of highly resolved chronologies. Here we reconstruct the erosion history of a small lake catchment in central Anatolia, located on the edge of one of the Mediterranean's most iconic badland landscapes in Cappadocia. Because these lake sediments are annually laminated, precisely dating clastic inwash layers and calculating recurrence intervals and flux rates is possible. Lake cores have been analysed for μXRF elemental geochemistry and via thin sections, along with proxies for hydroclimate (oxygen isotopes) and land cover (pollen). Peaks in titanium, along with other detrital elements, and changes in clastic layers indicate increased sediment influx into Nar Lake between 9300 and 8000 cal BP (ceramic Neolithic, when obsidian mining took

place nearby) and again, more importantly, during the last 2500 years (Iron Age to modern), the latter exhibiting three phases of enhanced catchment erosion. Multiproxy comparisons show that these phases were related primarily to periods of increased human impact on vegetation and soils around the lake. Most sediment influx has been in the form of turbidites, linked to the presence of a fan delta at the lake edge, although this store does not appear to have significantly delayed sediment delivery from eroding hillslopes to the lake bed. The marked increase in detrital influx during the late Holocene implies that badland development in the lake catchment is recent and largely anthropogenic, rather than ancient and of climatic causation, and probably involving stream capture. The record also shows that sediment influx diminished markedly at times when human land use disintensified, which in turn indicates that hillslope degradation is reversible with appropriate land management.

Keywords: Cappadocia; turbidites; lake; badland; erosion; Holocene; varves

1. Introduction

Human mismanagement has long been argued to have progressively pushed geomorphic landscapes towards an increasingly unsustainable disequilibrium (Marsh, 1864; Sherlock, 1922). This is most obviously manifest in badland terrain that is thought to provide visible testimony to landscapes *ruined* by deforestation and overgrazing. It applies especially in regions of long-standing human occupation, such as the Mediterranean, and it underpins the idea that there is a geomorphological expression to a human-dominated earth system, viz. the Anthropocene (Brown et al., 2017). On the other hand, debate is long-standing in historical geomorphological studies about the relative importance of natural drivers of erosion, such as climate change, versus human-induced land cover change (e.g., Wagstaff, 1981; Grove and Rackham, 2001). Karl Butzer made seminal contributions to these debates; for example, in highlighting how human-induced landscape degradation could be ancient (e.g., in pre-Hispanic Mesoamerica) and how the effects of land conversion and

climate change were often synergistic and consequently required cross-disciplinary investigation (Butzer, 1974, 2005).

Some of the most widely studied field evidence for past changes in soil erosion and sediment flux comes from downstream records of alluviation and incision in Mediterranean river valleys (e.g., Vita-Finzi, 1969; van Andel et al., 1990; Macklin and Woodward, 2009; Dusar et al., 2011). Dating and sedimentological analyses have enabled the creation of regional alluvial chronologies, and this led to the recognition that significant geomorphological changes have taken place during historical times. Among them is the Younger Fill of Vita-Finzi (1969), found in many Mediterranean valleys, and which formed during post-Roman times. While these studies highlight the widespread nature of historical slope destabilisation and soil loss, they have been less informative about their underlying causes. Vita-Finzi, for example, attributed his Younger Fill primarily to historic variations in climate (e.g., Medieval Climate Anomaly) rather than to post-Classical abandonment and subsequent lack of maintenance of agricultural terrace systems. In practice, alluvial records do not easily permit the kind of controlled field experiment conditions needed to establish clear causal relations. Fortunately, chronological precision and accuracy may be far better in some lake sediment records (Ojala et al., 2012; Vannière et al., 2013), and these also offer the possibility of testing different causal mechanisms via a multiproxy approach.

In the study presented here we reconstruct the erosion history of a small lake catchment in central Anatolia, located on the edge of one of the Mediterranean's most iconic badland landscapes in Cappadocia. Nar Lake has been monitored since 1998 (Jones et al., 2005; Woodbridge and Roberts, 2010; Dean et al., 2015a) and its Holocene hydroclimatic and vegetational history have been reconstructed from lacustrine sediment cores (Jones et al., 2006; England et al., 2008; Dean et al., 2015b; Roberts et al., 2016). Because the lake sediment cores are mostly laminated, it is possible to date clastic "flood" layers that are present in its sedimentary record and to calculate their recurrence intervals and sediment volumes rather precisely. In this paper, we present the results of μXRF geochemical core scanning, notably for detrital elements indicative of catchment erosion, along with analysis of clastic layers via thin

sections, granulometry, and other methods. These new data allow us to evaluate critically the long-term relationship between catchment erosion with (i) past climate variations and (ii) land cover change, as reconstructed using previously published proxy evidence from the same sedimentary archive. Finally, we compare our results to documented historical and archaeological records from the same region to ask 'how old are Cappadocia's badlands?'

2. Study area

Nar Gölü (Göl = Lake in Turkish; 38°20'25'' N, 34°27'24'' E; elevation 1363 m asl) is a >20 m deep oligosaline volcanic maar lake, ~0.5 km in diameter (Fig, 1). There is no surface outflow and the modern lake water is slightly saline (EC of 2.5-3.1 mS cm^{-1} and pH of 7.1-7.4; Dean et al., 2015a). The lake water is stratified, with low dissolved oxygen levels below ~8 m depth, except during the winter months. The lake catchment is small (~4 km^2 including the lake surface) but with ~240 m of relative relief in the drainage basin over a horizontal distance of <1 km, and upper catchment slopes steeper than 20°. The southernmost rim of the catchment has been eroded to form hoodoos (*fairy chimneys*) and the eroded sediments have created an alluvial fan delta on the southern side of the lake that extends deep into the lake waters (Fig. 1). There are no permanent surface water inflows but several ephemeral streams and also a number of geothermal and coldwater springs around the lake. Nar Lake is situated within the Central Anatolian Volcanic Province, and the faulting process that created the maar probably began in the middle-late Pleistocene (Gevrek and Kazancı, 2000).

The lake is located in the oak parkland zone that covers much of the Anatolian Plateau, and the region has a continental Mediterranean climate (see Dean et al., 2015a, for details). Agricultural activity in the catchment is minimal at the present day, with no permanent settlement inside the watershed, although there are abandoned fields on the northern side slopes, and also livestock grazing. Evidence of historical settlement within the lake catchment includes rock-cut dwellings that were likely occupied between the tenth and thirteenth centuries CE. Rock-cut churches and

underground cities are a characteristic feature of Byzantine Cappadocia, and one of the reasons for the region's designation as a UNESCO World Heritage site.

Figure 1: (a) Location map of Nar Lake and catchment, showing coring sites and area of badland; (b) oblique satellite image of lake and catchment (Google Earth); (c) representative core section from unit 1, showing varves interrupted by clastic layers (arrowed), one thick, the other thin.

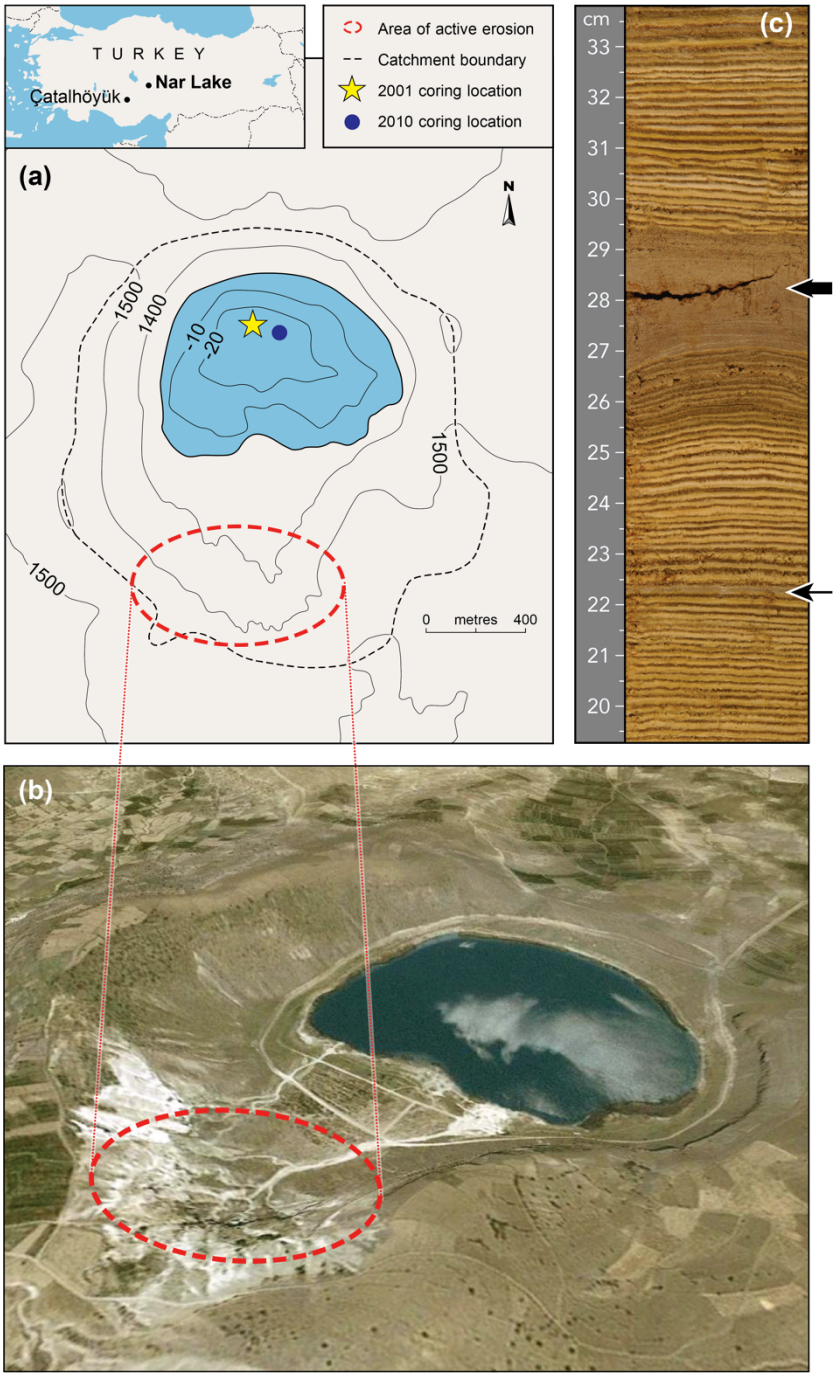

Central Anatolia contains an exceptionally rich and well-studied archaeological record (Table 1). The oldest excavated archaeological sites in Cappadocia date to the Aceramic Neolithic, notably at the protoagricultural settlement at Aşıklı Höyük (later ninth and early eighth millennia BCE). During this and the subsequent Ceramic Neolithic and Chalcolithic periods, Cappadocia provided the principal source of obsidian for central Anatolia and beyond, and several obsidian factories have been identified. One of them is on Nenezi Dağ, a hill located 3 km north of Nar Lake, just outside its catchment. Lithic artefacts and *débitage* are common in the vicinity of the lake, although no distinct occupation site has so far been found.

After a period of apparent demographic decline during the middle Chalcolithic, evidence from regional archaeological site surveys and excavations indicates a renewed increase in settlement during the third millennium BCE, corresponding to the Early Bronze Age (Allcock and Roberts, 2014). During the Middle and Late Bronze Age, central Anatolia lay at the heart of the expanding Hittite Empire that came to an end in the late second millennium BCE, when there was a major rupture in the regional socioecological system (Allcock, 2017). A new demographic cycle began during the first millennium BCE at the end of which Cappadocia became a Roman province (17 CE), with its capital at Caesarea (modern Kayseri). Two subsequent periods are especially well represented archaeologically, the first being the early and mid-Byzantine, and the second being the Selçuk period. A major episode of early Byzantine church building took place in the fifth and sixth centuries CE. However, this was followed by a period of increasing insecurity linked to Arab invasions between the mid-seventh and tenth centuries CE. A mid-Byzantine revival in the tenth and early eleventh centuries saw the creation of a series of remarkable mural paintings inside rock-cut churches (Ousterhout, 1999, 2005; Thierry, 2002). After this *Golden Age*, Byzantine rule in Cappadocia came to an end around 1080 CE, although Christian communities continued under Islamic Selçuk domination. The early Turkish Selçuk state was geographically centered in south-central Anatolia; after its collapse in 1299 following the Mongol invasion, Cappadocia eventually became part of the Ottoman Empire until the foundation of the modern Turkish Republic in 1923.

173 Table 1: Major historical and archaeological periods in central Anatolia

174

Period	Date	Further details
Turkish Republic	since 1923 CE	
Ottoman	~1450 to 1923 CE	
Medieval Turkic	1071 to ~1450 CE	principally Selçuk, 1071-1299 CE, Mongol invasions 1260s
Byzantine	330 to 1071 CE	early and middle periods separated by Arab wars (~640 to ~950 CE)
Hellenistic-Roman	331 BCE - 330 CE	
Iron Age	1200 - 331 BCE	includes Dark Age (1200-900 BCE) and Achaemenid Persian Empire (after 585 BCE)
Bronze Age	3000 - 1200 BCE	includes Early, Middle and Late Bronze Ages
Chalcolithic	6000 - 3000 BCE	
Neolithic	>8500 - 6000 BCE	includes Aceramic (pre-7000 BC) and Ceramic (post-7000 BC) phases

175

176

177 **3. Methods**

178

179 The late Holocene sedimentary record from Nar Lake was initially cored in 2001 and
180 2002 using a Livingstone type stationary piston corer. These cores (NAR01/02) span
181 the last ~1700 years and were analyzed at high temporal resolution for stable
182 isotopes (Jones et al., 2006; Dean et al., 2013), pollen (England et al., 2008), and other
183 proxies. In 2010, deeper lake coring took place at 21.5 m water depth from a platform
184 using a UWITEC stationary piston corer. At the main core site, triple overlapping
185 parallel cores were recovered in close proximity. These cores were opened, split in
186 two lengthways, described, and photographed, with half being kept as an archive. The
187 three core sequences were correlated visually at tie-points, and the best sections

from three parallel cores were spliced together to create a master sequence 21.69 m long (NAR10) that extends back to Late Glacial times.

A seismic survey of the lake bed and its underlying sediments was carried out in 2010 using a Boomer system, coupled to a high precision GPS. Fifty-three transect lines were made across the lake with an interval spacing of 30 m, east-west and north-south, to create a detailed bathymetric map and cross section profiles of the upper ~20 m of the lake sediments (Smith, 2010; Roberts et al., 2016). These highlight the morphology and internal sedimentary structures of the subaqueous fan delta on the south side of the lake.

The majority of the Nar Lake sediment cores are laminated, and most (if not all) of the laminations appear to be annual (i.e, varves), based on 20 years of lake monitoring (Dean et al., 2015a) and comparison with ^{137}Cs, ^{210}Pb, and other dating methods. For laminated parts of the core sequence, chronologies were established by layer counting by eye and in thin sections. Because some parts of the core sequence were not laminated (see Fig. 2), additional age estimates were required. These were provided by U-Th dating from two aragonite-rich layers at 1949 cm (11.82 ±0.52 ka) and 1021 cm (4.41 +0.16/–0.17 ka) using a total dissolution isochron approach (see Dean et al., 2015b, for further details; see Roberts et al., 2016 for age-depth curve). The first of these U-Th ages lies close to, and agrees well with, the stratigraphically inferred Pleistocene-Holocene boundary in the cores. The second U-Th date provides a fixed datum for the mid-Holocene part of the core record. These ages have been used to pin floating laminae counts for the early-mid Holocene. For nonlaminated parts, linear sedimentation has been assumed (note that ages are quoted in years before 1950). Lake waters have a modern ^{14}C age of ~15,000 years because of volcanic out-gassing, making this dating method inapplicable.

Sequential thin sections have captured an almost continuous record of *in situ* sediment deposition over the last 2.6 ka (unit 1) and during Neolithic times (sub-unit 5a). The methodology for thin section preparation largely follows Boës and Fagel (2005). For each thin section, 6 cm by 1 cm blocks of unconsolidated sediment were cut from the NAR10 split core and freeze-dried. Once dry, sediment blocks were

impregnated with epoxy resin (Araldite 2-component resin) under a gentle vacuum to minimise sediment disturbance of resin uptake. These resin-embedded sections were cut perpendicular to the varves' bedding plane, fixed to a microscope slide, and lapped down to a thickness of 20 μm. All thin sections were finished with a cover slip. The thicknesses of varve sublayers were determined using a microscope reticule on thin sections (e.g., Swierczynski et al., 2013). Measurements were made perpendicular to the laminae bedding plane, along a linear transect that bisects the core's width (Lamoureux, 2000), only deviating from the transect when the sediments' structure was significantly disrupted or damaged (Francus et al., 2002). The use of a petrographic microscope also enabled the composition and structure of sublayers to be determined.

The elemental geochemistry of the NAR10 cores was measured using Itrax X-ray fluorescence (μXRF) core scanning (Croudace et al., 2006; Rothwell and Rack, 2006). Scanning was carried out on cut half-cores at Aberystwyth University in November 2010, using a Cox Analytical Systems scanner at a 200-μm sampling interval resolution (400 μm for nonlaminated sections; for details see Allcock, 2013). One drawback of Itrax scanning is that accurate analysis of lighter elements is difficult to achieve (e.g., Mg). They can, however, be detected with handheld XRF analysers (Kylander et al., 2011). The cut NAR10 core master sequence, along with soil/sediment samples from the lake catchment, were therefore also analysed using a Thermo Scientific Niton XL3t GOLDD series XRF hand held scanner with helium purge at Plymouth University. A sampling resolution of every 8 cm was used for the core scanning with the 3 mm small spot selected (Allcock, 2013). The catchment samples were analysed in sample pots using the handheld instrument in its countertop test stand. By using the two XRF techniques together, a broader array of elements was determined and cross-correlations could be made to ensure that ITRAX readings are an accurate reflection of geochemical variations in the Nar Lake sequence.

Varve deposition in the lake is driven by seasonal changes (Jones et al., 2005; Primmer, 2018). Following winter when the lake is thermally mixed, the onset of lake stratification in early spring is associated with enhanced autochthonous productivity and an algal bloom, often of diatoms. This increases lakewater pH, via the

photosynthetic consumption of CO_2, and combines with an increased evaporation/precipitation ratio to cause carbonate supersaturation and authigenic precipitation of calcite and/or aragonite in late spring or early summer (Dean et al., 2015a). The resulting white carbonate layer is succeeded by a dark-coloured mix of organic matter, diatom frustules, and some diffuse clastic material, representing late summer, autumn, and winter deposition. This regular seasonal cycle of mainly authigenic sedimentation is periodically interrupted by discrete and distinct clastic layers of variable thickness, notably in the upper ~6 m (unit 1). These clastic layers have been dated by varve counting, measured and sampled in the NAR01/02 and NAR10 core series. The clastic layers are also identifiable (in the NAR10 series only) via Itrax data. The Itrax XRF log shows that clastic layers are well identified by K and Ti increases, while Ca concentration remains low. Thus, to separate the clastic layers from the background, we selected the K/kcps and Ti/Ca signal.

In order to create a time series of individual clastic layers we have processed the data statistically, following the principles used for reconstruction of fire-event frequency (Vannière et al., 2008) and flood frequency (Vannière et al., 2013). The low-frequency trend, estimated by calculating the moving first quartile with a running window of 1000 values, was removed in order to normalise the signals. The normalisation corresponds to the reduced value (raw value minus the mobile quartile) divided by the mobile standard deviation: (Kkcps) normalised = (((Kkcps) raw - (Kkcps) mobile quartile1) / (Kkcps) mobile standard-deviation). This normalised signal has two components: first, the background, which oscillates around zero; and second, the peak component, with the latter being significantly different from the background. Two populations of values are usually present with the lowest ones interpreted as analytical noise, while the highest positive ones above the threshold value (TV) are assumed to represent intrusive events. A Gaussian mixture model was used to decompose the peak component: that is, to analyse the histogram plot of the peak-component frequency distribution and to choose the TV (MIXMOD Software; Biernacki et al., 2006). By using this model two overlapping subdistributions can be disentangled and the upper limit of the main distribution identified, which may potentially be the upper limit of the analytical noise-related variation. Time-series analysis of the peak components then allows reconstruction of event frequencies. We

evaluated the distribution of peaks along the sequence by smoothing the sum of episodes with a 50-year moving time window. Variations in average and total clastic layer thickness are also presented per 50 years.

Particle size analysis of clastic layer sediments was carried using a Mastersizer 2000 laser diffraction system, after sieving to remove any particles >1 mm in diameter. The methods used for stable isotope analysis of endogenic carbonate and pollen have been described in previous publications (Jones et al., 2006; England et al., 2008; Dean et al., 2015b).

4. Results

The combined NAR01/02 and NAR10 core record covers the last 13,800 years (13.8 ka) from the Late Glacial Interstadial to the present day (Dean et al., 2015b; Roberts et al., 2016), although U-Th dating and varve counting suggest a gap in sedimentation between 6500 and 5000/4500 cal BP, at 1139 - 1161 cm (the unit 3/unit 4 boundary). The NAR10 cores have been subdivided into seven lithostratigraphic units as described in Table 2.

Negative $\delta^{18}O$ values on endogenic carbonate, high Ca/Sr ratios, and the presence of laminated (i.e., deepwater) sediments indicate climatically wet phases during the early–mid Holocene (especially 11,700-9500 and 8000-7000 cal BP) and again from 1500 to 600 cal BP (Fig. 2). By contrast, peaks in Mg, positive $\delta^{18}O$ values, elevated diatom-inferred salinity, and an absence of laminated sediments indicate markedly dry hydroclimatic conditions during the Late glacial Younger Dryas stadial (~12,900-11,800 BP), and again at times between 4300 and 2600 cal BP. Pollen evidence indicates a gradual increase in woodland at the start of the Holocene, to create an oak parkland vegetation that persisted until Bronze Age times, when there was a sharp decline in woodland cover, probably a combined result of human deforestation and a trend toward climatic desiccation. During the last 2500 years (NAR10 unit 1), pollen evidence clearly indicates agricultural land use in the surrounding region, including the so-called Beyşehir Occupation phase, with tree crops, ruderal plants, and cereal-type pollen (England et al., 2008; Roberts, 2018; Woodbridge et al., 2018).

320

321 Table 2: NAR10 lithostratigraphic units

322

Unit	Depth cm	Inferred age (yr BP)	Summary description
1	0 - 592.7	-60 to 2520	mm thick laminated silts, with frequent grey clastic layers
2	592.7 - 753.7	2520 to 3700	Mostly non-laminated with occasional thin laminations. Frequent hard nodular layers
3	753.7 - 1138.7	3700 to >4500	Thick laminations, some massively deformed. Probable hiatus at base of unit
4	1161.2 - 1428.2	6541 to 8190	Very finely laminated, pale beige marl
5	1428.2 - 1974	8190 to 11,830	mm thick olive-beige laminations, some clastic layers in sub-unit 5a
6	1974 - 2013	11,830 to ~12,840	Homogenous non-laminated grey marl. Equivalent to Younger Dryas
7	2013 - 2169	~12,840 to ~13,800	Laminated silts with some abrupt colour changes

323

324 The overall rate of sedimentation in the NAR10 cores has been relatively constant for
325 most of the Holocene at 1.5 mm y^{-1}, although it increased to 2.3 mm y^{-1} in unit 1 (Fig.
326 2). Compression loading and dewatering may account for some of the apparent
327 increase in sedimentation rate in the last ~100 years. The main exception to the long-
328 term trend occurs in unit 3, dating to the second millennium BCE (fourth millennium
329 BP). Laminations between 798 and 1100 cm are much thicker than in the rest of the
330 cores; if these are annual, as laminae counts and U-Th age estimates suggest, then this
331 implies a fourfold increase in gross sedimentation rate for this interval to 5.8 mm y^{-1}
332 (see section 5 for further discussion). The sedimentation rate appears to have been
333 lowest during NAR10 unit 6 (0.4 mm y^{-1}), corresponding to the Younger Dryas stadial
334 when the climate was cold and dry.

335
336 Aside from the relatively constant overall rate of sedimentation, Itrax data show
337 significant downcore changes in the influx of detrital clastic elements such as Ti, Fe, K,
338 and Rb into Nar Lake. These elements show very similar patterns and close
339 correlations to each other in the NAR10 cores (Allcock, 2013). Modern soil/sediment
340 samples from the lake catchment are dominated by Si along with Fe and Al (Allcock,
341 2013, p. 127), elements that exist predominantly in detrital (i.e., minerogenic)
342 sediments. In the core, however, there is a very significant component of biogenic Si,
343 notably in the form of diatom frustules, which makes Si less useful as a direct erosion
344 indicator than the ratio between Ti and Ca along with K/Kcps concentrations.
345 Titanium (Ti) rather than Al is used for normalization of terrigenous input because Al
346 is a relatively light element that is less accurately detected by Itrax. The Ti/Ca ratio
347 has been shown to be a good indicator because it is little affected by core variability
348 and water content under scanning film (Hennekam and de Lange, 2012). Elevated
349 Ti/Ca ratios and K values occur during two main times during the Holocene, namely
350 during unit 5a (9.3-8.0 ka cal BP; ceramic Neolithic) and again – more importantly –
351 during unit 1, dating to the last 2600 years (Fig. 2). In unit 1, there are large
352 amplitudinal fluctuations in K/Kcps values and the Ti/Ca ratio, associated with the
353 presence of discrete clastic layers. Itrax erosion proxies are lowest during unit 4,
354 dating to the early-mid Chalcolithic period (8.0-6.5 ka), at which time almost no input
355 of detrital sediment entering Nar Lake from its catchment is detectable.
356
357

Figure 2: Stratigraphy of the full NAR10 core sequence, sedimentation rate (overall rate and clastic input alone), Itrax profiles for detrital indices (Ti/Ca and K), hydroclimate proxies (Ca-Sr, Mg, and $\delta^{18}O$), and deciduous oak pollen percent (data partly from Roberts et al., 2016).

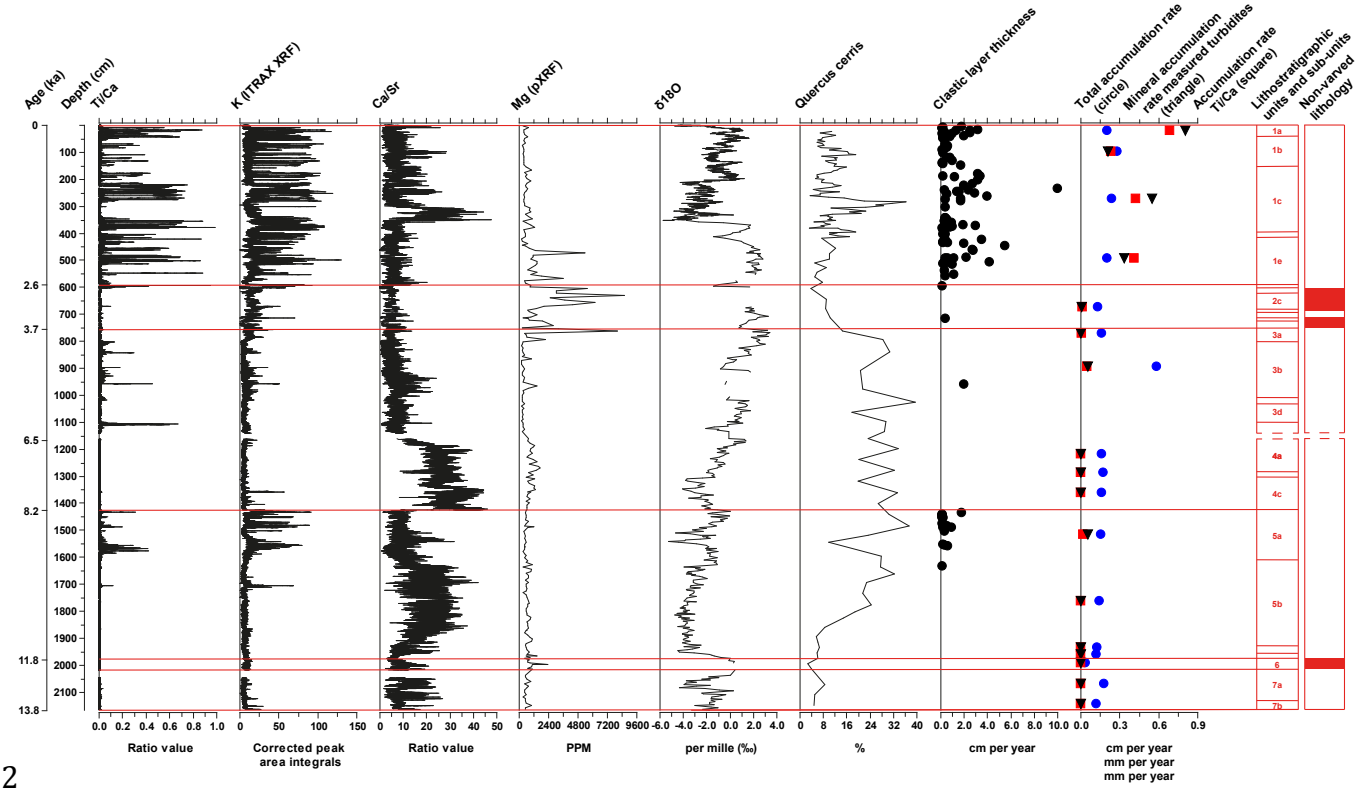

For clastic layers in the NAR10 cores, we can compare Itrax data with visual measurements of layer thickness and age. As Table 3 shows, there are some differences between these different measurement techniques in the number and thickness of layers recorded. Itrax scanning had a 200-µm measurement resolution, allowing the identification of layers as thin as 0.2 mm. By contrast, visible measurements were restricted to layers at least 1.0 mm thick. This resolution was increased by the use of thin section microscopy that has revealed the typical composition of nonseasonal clastic layers: a well-mixed mass of terrigenous clasts, inwashed obsidian, along with some organic detritus and calcareous material. Clastic sublayers characteristically display abrupt stratigraphic boundaries, indicative of a rapid transition to the dominant depositional process, typically associated with an individual depositional event (Mangili et al., 2005). With their high concentration of allogenic sediment, these inwash sublayers are visually distinct from the varves' sub-

layers of carbonate and organic material. Thin section analysis indicates that while these non-seasonal sublayers can be located at any position within the varve cycle, the majority (67%) were deposited between the organic and carbonate sublayers. Given that the seasonal deposition endogenic carbonate typically occurs during the early summer (Dean et al., 2015a), these clastic layers may have been deposited during the preceding months (March-May). These months reflect the wettest period of the year, accounting for ~35% of the site's annual precipitation and much of the seasonal snowmelt.

The difference in measurement resolution means that Itrax- and thin section-derived data show substantially more layers during unit 1 and with a mean layer thickness only about half that for visible measurements; analysis also shows some differences between K/Kcps and Ti/Ca. Nonetheless there is good agreement in the timing of layer events between the two Itrax indices and also between these and the visible and thin section measurements. Almost all of the main clastic layers can therefore be recognised across the different measurement techniques.

Replicate records of the clastic layers in two independent core sequences (NAR01/02 and NAR10), both located in the deepest part of the lake (Fig. 1), make it possible to assess their spatial extent and variability for the last 1500 years. There is good accordance in the overall timing and magnitude of clastic layers in the two core sequences (Fig. 3), with a concentration of events in three time intervals, namely (i) prior to 1340 cal BP (before 610 CE; phase 3), (ii) between 1036 and 664 cal BP (914-1286 CE; phase 2) and (iii) since 1920 CE (phase 1). Minor differences (typically ± 10 years or less) exist in the age of individual layers between the two cores, primarily the result of dating imprecision by varve counting. The biggest difference between the two core sequences is that clastic layers are ~60% thicker on average in the NAR10 than the NAR01/02 cores, implying lateral variation in the thickness of individual layers within the lake.

Table 3: Summary measurements of clastic layers for the last 1500 years in two Nar Lake sediment core records using different methods. Total sediment thickness for this time interval is 383 cm (NAR10) and 336 cm (NAR01/02)

	NAR10				NAR01/02		
	All layers		Layers ≥ 1mm		All layers		
	K/Kcps (Low)	Ti/Ca (Low)	K/Kcps	Ti/Ca	Thin section	Visual measurement	
total thickness cm	106.94	57.18	66.62	50.58	116.75	79.0	45.4
mean thickness cm	0.55	0.67	2.38	2.11	0.83	1.16	0.73
number of layers identified	196	85	28	24	141	68	62

Particle size analysis of the clastic layers shows that they are primarily silt sized, and analysis of subdivided samples from six layers from the NAR01/02 indicates that their lower part contains more sand (12.3%) and less clay (7.9%) than the upper part (5.2% sand, 11.9% clay); i.e., they display a fining-upward sequence. A similar trend was found in 22 of the thickest clastic layers in the NAR10 cores (Barnett, 2016), which also revealed that most of the change in granulometry within each clastic layer occurred in the basal 1 cm. Upward fining of grain sizes, indicative of gravitational sorting (Mangili et al., 2005), was also visible in thin sections of the thicker clastic layers. This would be consistent with higher-energy deposition and significant lateral sediment movement during the initial phase of event deposition, followed by lower-energy fine-grained sedimentation from the overlying water column.

Figure 3: Clastic layer thickness and age, last 1500 years; (a) NAR10 cores comparing measurement by Itrax scanning and visual recording; (b) comparison of visual and thin-section measurements, (c) visual measurements for NAR10 vs. NAR01/02 cores (note difference in vertical scale). Timescale in years before 1950 CE.

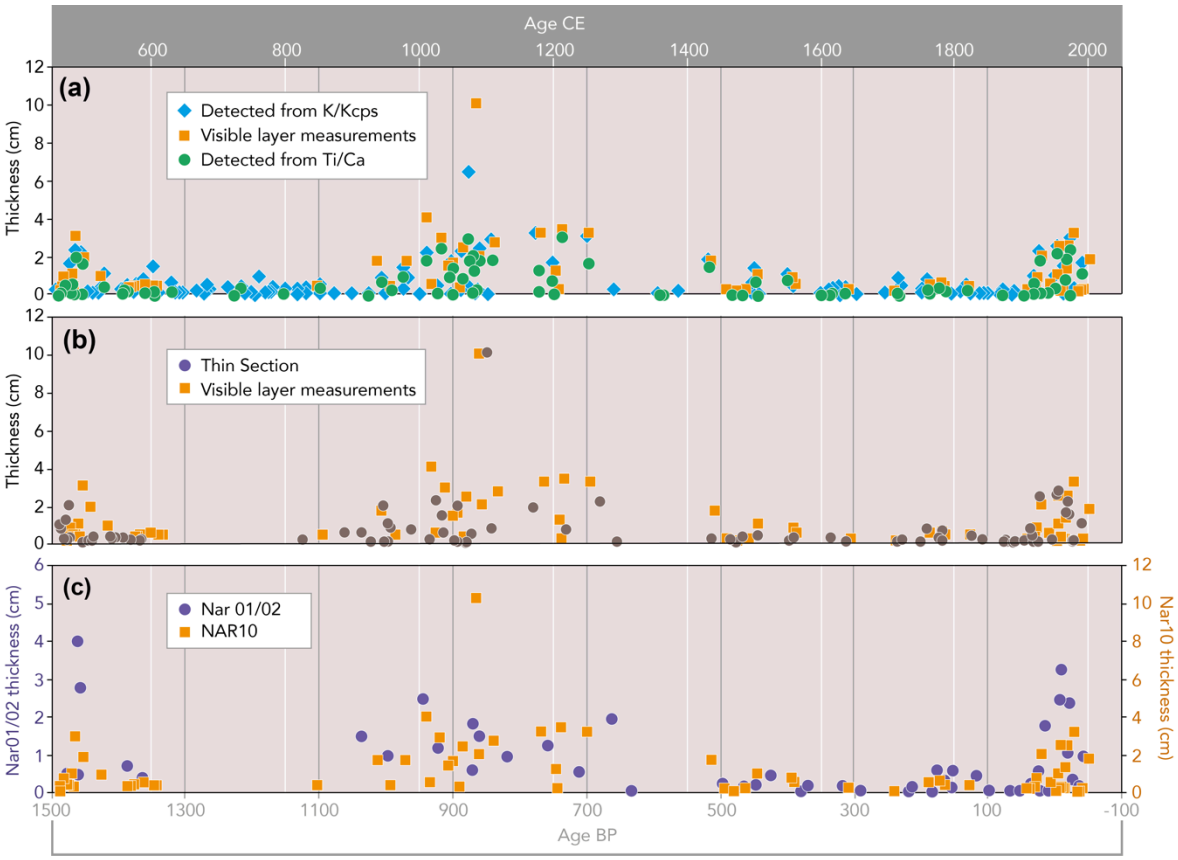

5. Discussion and analysis

5.1. Origin of clastic layers

Clastic sedimentation, aside from that at the margins, is deposited by two main mechanisms in lakes: first, dispersal as plumes of suspended sediment and thus suspension fall out, typically following an episode of particulate inwash; and second, transportation of material via density currents (Sturm and Matter, 1978). This transportation of material in a subaqueous environment occurs via turbidity currents, turbulent mixtures of sediment and water that deposit graded beds, or turbidites (Mulder et al., 2003). Turbidites comprise a fining upward sequence that represents a

waning of discharge as it spreads out farther away from the source of the current (Gilli et al., 2013). They occur anywhere that has a supply of sediment and a slope, and they are particularly common in deep lakes (Nichols, 2009).

Turbidites found in lake sediments can be initiated by failure of sediments on slopes creating turbidity currents, or alternatively, sediment-rich hyperpycnal flows driven by high volume runoff from inflowing rivers and streams (Osleger et al., 2007). Hyperpycnal flows occur when the density of subaerial discharge is higher than the density of the water in the lake or sea that they enter (Mulder et al., 2003). The result of these sediment-laden flows is deposition of a particular type of turbidite termed hyperpycnites. Turbidites can also form as a result of mass movements of a large buildup of sediment on slopes of a delta front that can fail as a result of earthquakes or delta collapse linked to lake-level fluctuations (Gilli et al., 2013). Challenges exist in differentiating between hyperpycnites and normal turbidites as they both display a similar facies succession and ultimately form as the result of high volumes of sediment entering the lake catchment.

Most of the thicker (>5 mm) clastic layers in the Nar sediment cores display a fining-upward succession, with a general trend of decreasing grain size through the layers. This and other characteristics suggest that the thicker layers originated via episodic turbidity flows within the lake, and we therefore interpret them as turbidites. What is less clear is whether they were triggered by high runoff during major flood events following storm events or rapid melting of winter snow cover, or whether they were initiated by nonclimatic factors, such as earthquakes. Cappadocia is located in a region of Anatolia with relatively low seismicity, although any volcanic activity would have the potential to cause harmonic earth tremors.

The internal structure and the presence of clay in the Nar turbidites indicates a degree of homogeneity that is more typically associated with mass movement processes associated with deltaic collapse rather than hyperpycnal flows caused by high intensity floods (Blass et al., 2005; Gilli et al., 2013). This would have potentially involved an autocyclic process of sediment buildup on the fan delta, overloading of the delta front, followed by slope failure. Similar conditions for turbidite formation

are seen in Lake El'gygytgn in Siberia (Juschus et al., 2009; Sauerbrey et al., 2013). Whatever their precise causal mechanism, the existence of an alluvial fan delta has created a temporary sediment store within the lake catchment, with the possibility of a temporal-spatial decoupling in sediment delivery between the point of slope erosion and deposition on the lake bed.

The thinner (<1 mm) clastic layers may represent flood inwash events rather than turbidites, while those between 1 and 5 mm are likely to be a combination of the two processes. Based on Itrax data for unit 1 (last 2500 years), normal palaeo-flood layers account for at least 30-40% of all depositional events. On the other hand turbidites, although probably less numerous (i.e., frequent), account for the majority of the clastic layers in terms of total thickness and sediment volume (table 4).

In addition to climate and land cover, sediment delivery to the lake has been influenced by the interaction between lithology, base level, and stream capture. Most of the active headwall gullies have eroded into fine-grained volcanic sediments, white in colour (and hence clearly visible on satellite imagery), and transported to the lake as suspended sediment. Slope breaks in the catchment reflect lithological changes and once any headcutting gullies breached the contact with the fine-grained volcanics there would potentially be a stronger clastic sediment signal in the lake. The streams feeding the fan delta would have incised their channels at times of falling lake levels, and these incisions would have then progressively worked headwards. The last major period of lake-level drawdown occurred between 4200 and 2600 BP, when the water depth was insufficient to maintain lake stratification and allow varve formation (Fig. 2). In turn this may have prompted an increase in headwall gully erosion. With rising lake levels (as occurred around 2600 BP, when varve formation recommenced), more sediment would have been stored in the fan delta, but also with potential for slope failure on the delta front.

There is evidence of expansion of the Nar Lake catchment by stream capture (see Fig. 4), which must have taken place during the late Holocene. Nar base level is currently 70 m lower than the tributary base level (in the adjacent river valley), so providing the framework for the capture. As the upper gullies captured drainage, they would

have increased water yield and sediment discharge to Nar Lake. As more of the captured catchment is in the weaker lithology, the sediment-to-water ratio would have increased leading to peak floodwater discharges being not only larger but more sediment-laden (Stokes et al., 2002).

Table 4: Frequency and importance of different types of clastic layers, based on thickness class, using Itrax data for unit 1

	K/Kcps (High)		Ti/Ca (High)	
thickness class	n	total thickness cm	n	total thickness cm
≥5mm	94	140.74	57	86.62
	19%	68%	22%	75%
1mm-5mm	252	55.1	116	23.16
	51%	27%	45%	20%
<1mm	146	9.56	87	5.68
	30%	5%	33%	5%
total	492	205.4	260	115.46

Figure 4: 2018 Google Earth CNES/Airbus image highlighting (yellow) the area of probable stream capture.

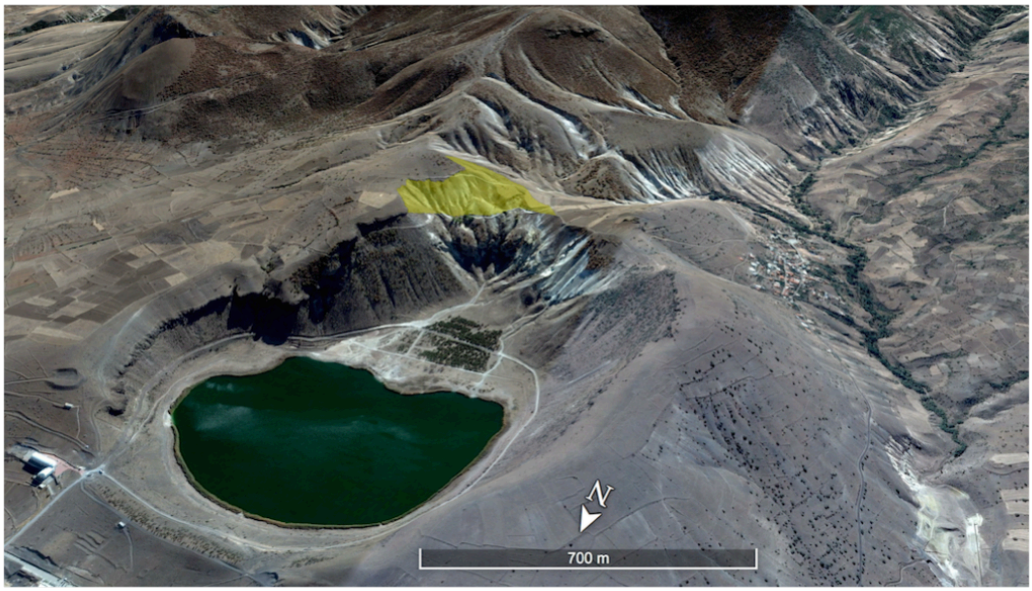

522

523 *5.2. Neolithic erosion*

524

525 Between ~13,800 and 9300 cal BP (1584 cm) influx of clastic matter into Nar Lake
526 was minimal, notwithstanding major changes in hydroclimate and vegetation during
527 the Late Glacial-Holocene transition. The Younger Dryas period was characterised by
528 particularly slow sedimentation and very low values for Ti/Ca and K. The time period
529 between 9300 and 8000 cal BP saw the first evidence of significant catchment
530 erosion, indicated by the presence of visible turbidite layers and in Itrax profiles (Fig.
531 2). This period can be subdivided into an early phase (1584-1550 cm; 9300-9165 cal
532 BP), with only three turbidites but elevated values of K and, especially, Ti/Ca, and a
533 later phase in which turbidite layers are more common (1506-1426 cm; 8830 to 8200
534 cal BP). The earlier phase was therefore characterised by catchment disturbance but
535 only rare turbidity flows. This was possibly because the alluvial fan delta had not yet
536 fully formed, so that eroded sediment could pass directly from the catchment into the
537 lake, without intermediate storage. By the later period, the presence of clear
538 turbidites and sharp peaks in detrital indicators indicate that a fan delta must have
539 been in existence. In this scenario, the current fan delta would have formed during
540 the early Holocene, and the initial lack of turbidites may signal the absence of a
541 sublacustrine delta front where these would be generated.

542

543 In terms of causal mechanisms, three potential explanations suggest themselves for
544 the period of early Holocene enhanced hydrogeomorphic instability. First, there is
545 evidence of a major eruption of one of Cappadocia's stratovolcanoes at around 8600
546 cal BP (Mouralis et al., 2002; Zanchetta et al., 2011; Schmitt et al., 2014), which may
547 have caused an influx of atmosphere-derived tephra. This would equate to ~1490 cm
548 depth in the NAR10 core sequence. Because the lake lies in a volcanic maar, it is not
549 easy to distinguish distal (extracatchment) from proximal (intracatchment) sources
550 of pyroclastic sediment in terms of their geochemistry. However, any volcanic input
551 would have been short-lived, and it did not disturb lake stratification or varve
552 formation, although co-seismic activity may have been responsible for microfaulting
553 of the sediments in unit 5a. Volcanic activity therefore cannot explain the longer-
554 term (~1300 year) increase in clastic influx.

555

556 A second, and more likely, potential cause is climatic. While the early Holocene as a
557 whole was a period of favourable climate and lake water balance, this was
558 interrupted by drier phases, initially around 9300 cal BP and then, more importantly,
559 after 8600 cal BP, culminating in the 8200 cal BP arid event. These hydroclimatic
560 changes are recorded in stable isotope and Ca/Sr data from the NAR10 cores and also
561 in δ^2H values of lipid biomarkers preserved in pottery from the Neolithic site of
562 Çatalhöyük (Roffet-Salque et al., 2018). The earlier phase of enhanced erosion also
563 saw a sharp, but short-lived, decline in oak pollen and a corresponding increase in the
564 pollen of ruderal plants such as *Rumex* (dock; see also Roberts et al., 2016). However,
565 this evidence is currently based on a single pollen sample and could have been
566 anthropogenic as well as climatic in origin. Aridification trends seem likely to have
567 contributed to Neolithic landscape instability, especially around 8.2 ka, which
568 coincides with the thickest early Holocene turbidite layer. On the other hand, climate
569 alone seems unlikely to be a sufficient explanation, as other climatic transitions
570 toward aridity during the Late Quaternary record from Nar (e.g., onset of the Younger
571 Dryas and of the megadrought at ~3.2 ka cal BP) are not accompanied by any
572 increase in erosion.

573

574 Third, human-induced disturbance may have contributed to Neolithic erosion in the
575 Nar Lake catchment. The period between 9300 and 8000 cal BP coincides with the
576 Neolithic occupation at Çatalhöyük East Mound, the largest known settlement of this
577 period in Anatolia (Hodder, 2014). One of the main sources of the obsidian found at
578 Çatalhöyük is Nenezi Dağ, a hill located 3 km from Nar Lake, just outside its
579 catchment (Carter, 2011). This obsidian workshop was active throughout the
580 ceramic Neolithic period, especially from 8600 to 8200 cal BP, probably on a seasonal
581 basis. Nar Lake would have provided an obvious base for people mining the black
582 volcanic glass, with freshwater springs around the lake providing a year-round water
583 source for livestock as well as human use. One of the principal freshwater springs lies
584 at the base of what is today eroding badlands. Nenezi obsidian was also used at the
585 slightly earlier, but geographically closer, aceramic Neolithic settlement sites of
586 Musalar and Aşıklı Höyük (Kayacan and Özbaşaran, 2007; Balcı, 2010). A comparison
587 of proxies for climate, erosion, and obsidian mining (Fig. 5) shows that the period

8600-8200 cal BP was marked by an increase in the share of Nenezi Dağ obsidian used at Çatalhöyük, corresponding to the main phase of Neolithic turbidite deposition. The same period was also characterised by a trend toward climatic aridity. Hence, it seems probable that this period of landscape instability resulted from climatic and anthropogenic factors operating in combination.

Figure 5: NAR10 Neolithic changes in erosion (clastic layer thickness in cm, left axis scale) and climate (right axis), along with proportion of Nenezi obsidian found at Çatalhöyük (left axis scale; data from Carter, 2011).

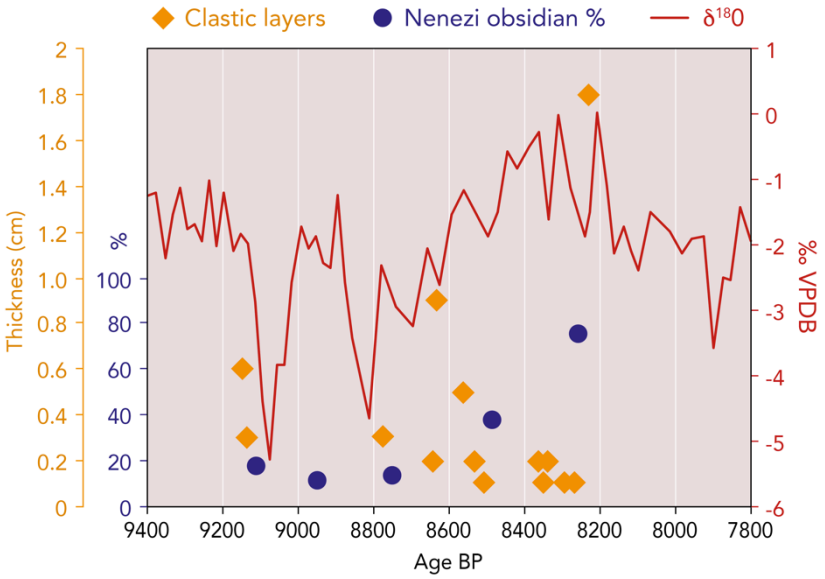

5.3. Late Holocene erosion history

Apart from a single turbidite layer at the time of the 4.2 ka cal BP drought event (962 cm) and another around 3.5 ka cal BP (718 cm), no other post-Neolithic clastic layers are recorded in the NAR10 core sequence until sedimentary unit 1. This implies geomorphologically stable terrain with only limited erosion in the lake catchment for most of the mid-Holocene, notwithstanding the fact that this period saw major changes in climate, vegetation cover, and lake level, along with the development of complex societies. Itrax detrital indices indicate minimum levels of clastic input into the lake in unit 4 (8000-6500 cal BP, early-to-mid Chalcolithic), showing that any badland development initiated in the preceding Neolithic period had been arrested

and the landscape had healed. Units 3 and 2 (~4500-2600 cal BP) included periods of drought and low lake levels, and also a major decline in woodland cover, attested by lower oak pollen percentages. Even so, the increase in clastic input to the lake, according to Ti/Ca ratios and K concentrations, was modest until 2500 cal BP (unit 1). During the time period before this, the Nar sequence stands in contrast to some other records of erosion history in central Anatolia. In tributary valleys of the middle Sakarya River near Gordion, for example, soil erosion rates started to rise in Late Chalcolithic or Early Bronze Age times (i.e., 5500-4000 cal BP; Marsh and Kealhofer, 2014). Similarly, topsoil-derived alluvium (the Upper Alluvial Complex) began to be deposited on the Çarşamba alluvial fan in the Konya basin during Bronze Age times (Boyer et al., 2006; Ayala et al., 2017). On the other hand, the increase in inferred hillslope erosion at Nar after 2500 cal BP is similar in date to that recorded from the Gravgaz depression (Dusar et al., 2012). An increase in minerogenic sediment influx is also recorded during the first millennium BCE at Gölhisar, similarly located in southwest Anatolia (Eastwood et al., 1999).

During unit 1, influx of clastic sediment increased markedly, rising from <1% to >39% of the total accumulated sediment (Fig. 2). A total of 97 clastic layers were recorded visually in unit 1 of the NAR10 cores, representing one event per 27 years, while Itrax and thin-section data record a larger number of mainly thin (typically <2 mm) layers. Clastic layers occur throughout the ~6 m of unit 1 in the Itrax data, with the only significant multidecadal periods of nondeposition being at 1893-1838, 842-775 and ~700-600 cal BP.

The results of signal processing to generate flood event frequencies and magnitudes per 50 years are shown in Fig. 6. Event frequencies reached a maximum at 1800 cal BP and then declined to reach a minimum at 750 cal BP before gradually rising again toward the present day (Fig. 6a). The thicker (≥5 mm) turbidite layers were much less evenly distributed through time than the thin flood layers, with distinct event clusters and intervening time gaps (Fig. 3). This uneven temporal distribution is significant, as it shows that the main turbidite layers were not simply the consequence of an autocyclic process of sediment buildup and fan slope failure. Instead, they must have been controlled primarily by exogenous (catchment) rather

644 than endogenous (within-lake) processes. Average layer thickness per 50 years
645 peaked between 1050 and 650 cal BP (Fig. 6b), including the single thickest turbidite
646 layer in the whole core sequence (~10 cm), which dates to 878/868 cal BP (1077±5
647 CE). This is coeval with dates for the rockcut features in the Nar catchment during the
648 mid-Byzantine *Golden Age*. By combining layer frequency and thickness, temporal
649 changes in total volume of clastic influx into Nar Lake can be calculated (Fig. 6c). This
650 shows three main periods of elevated detrital input from the lake catchment during
651 the last 2500 years, namely 2050-1350 cal BP (phase 3), 1000-700 cal BP (phase 2),
652 and since 50 BP (i.e., since the beginning of the twentieth century, phase 1). The first
653 of these phases displays a cyclical pattern, with three influx peaks separated by
654 intervening troughs (i.e., phases 3a, 3b, and 3c).
655
656 Figure 6 (a) Clastic layer frequency, (b) individual clastic layer thickness, and (c)
657 total clastic layer thickness per 50 years, since 2500 cal BP in the NAR10 core
658 sequence.
659

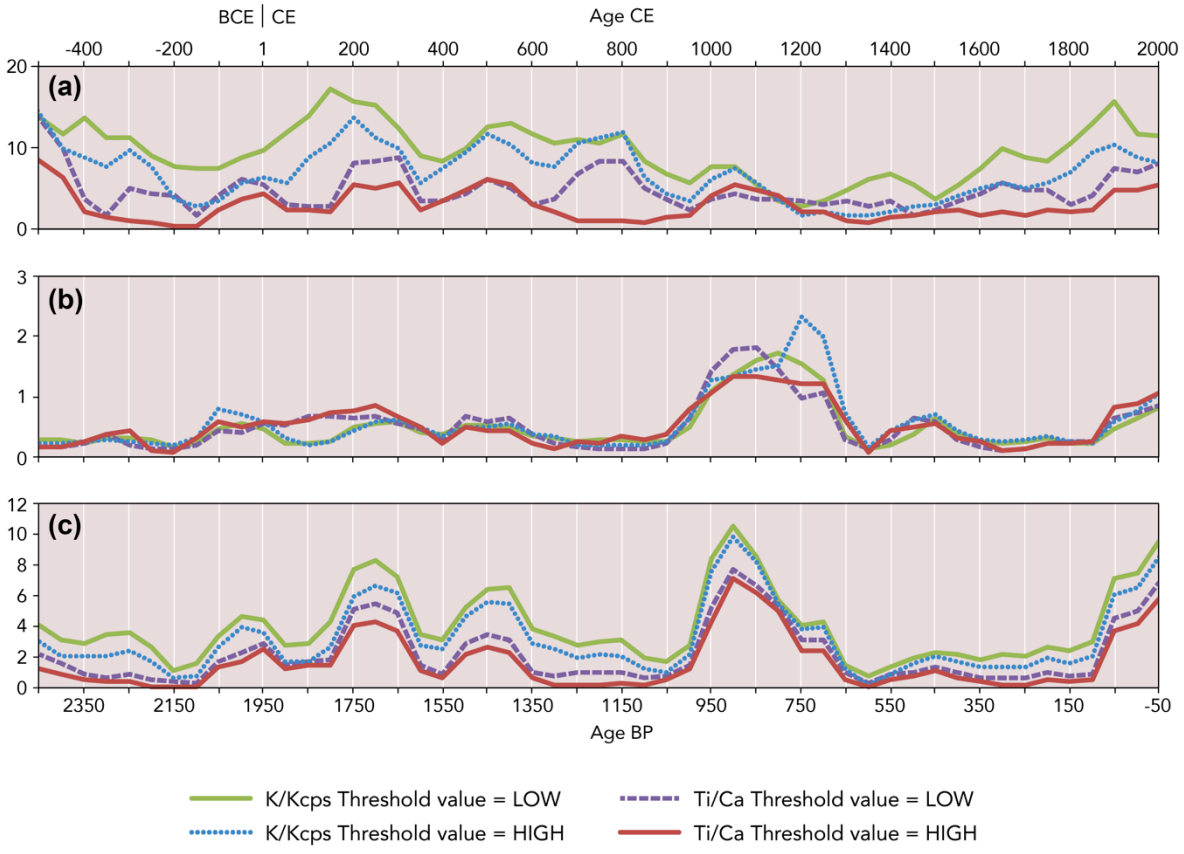

660
661

Multiproxy comparison can be used to investigate the causal mechanisms behind deposition of clastic layers in Nar Lake during the last 2500 years. As these different proxies derive from the same lake sediment cores analysed for clastic layers, there is no risk of temporal miscorrelation between them. For climate we use $\delta^{18}O$ on authigenic carbonate, with more negative isotopic values indicating wetter hydroclimatic conditions (Jones et al., 2006; Dean et al., 2015b). The $\delta^{18}O$ data indicate drier conditions before 1500 cal BP, followed by a period of overall wetter climate from 1500 to 600 cal BP, including the Medieval Climate Anomaly. During the Little Ice Age (after 600 cal BP/1400 CE), regional hydroclimate was once again drier, before a shift to wetter conditions during the mid-twentieth century (Fig. 7). Because the mean residence time of water in this nonoutlet lake is around 11 years (Dean et al., 2015a), $\delta^{18}O$ data provide decadal-average, not annual, conditions, and they are unlikely to sense individual hydroclimatic events, such as high-intensity storms.

Land cover can be inferred from pollen analysis (England et al., 2008), with agricultural land use indicated by the proportion of Cerealia-type and olive tree pollen. There was an important phase of olive (*Olea*) cultivation between ~1900 and 1300 cal BP, during Imperial Roman and early Byzantine times. Forest cover is recorded by the percent pollen of deciduous oak (*Quercus*), which peaked between 1300 and 1000 cal BP (Fig. 7). This period of reforestation and rewilding coincides historically with the period of the Byzantine-Arab wars, when central Anatolia became a frontier zone and was depopulated. Pollen recruitment was not restricted to the lake catchment but captured regional to extraregional as well as local pollen. The presence of cereal-type pollen in the sediment cores, for example, does not necessarily mean that cereal crops were being cultivated within the lake watershed, although they must have been grown close by.

Figure 7: Clastic layers in NAR10 vs.proxies for hydroclimate ($\delta^{18}O$), human land cover change (pollen), total and individual clastic layer event thickness. Stable isotope data from Jones et al. (2006) and Dean et al. (2015); pollen data partly from England et al. (2008). Shaded bands show the main periods of enhanced erosional influx into Nar Lake.

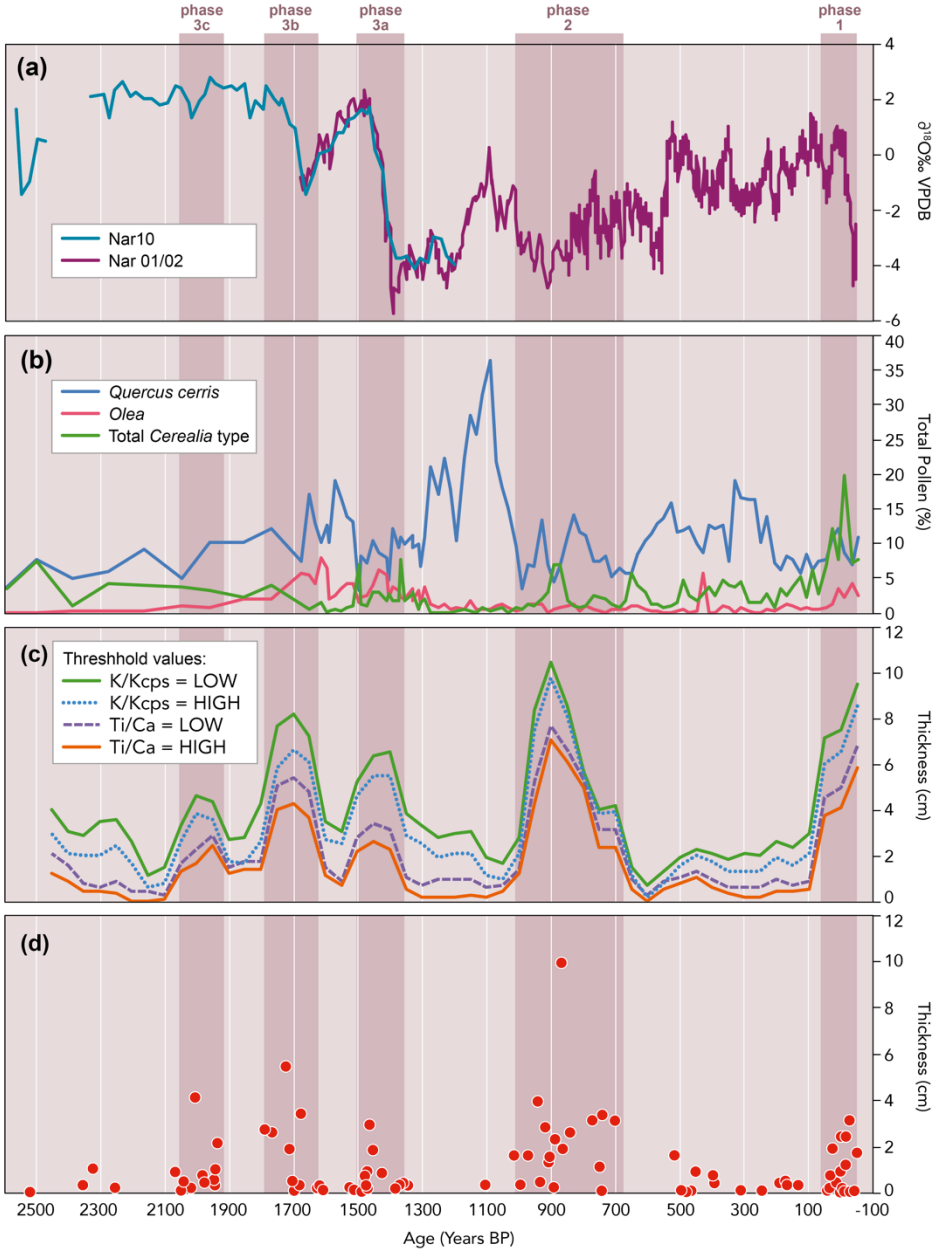

Long-term trends in the frequency of clastic layers (Fig. 6) show no obvious correspondence to either $\delta^{18}O$-inferred climate or pollen-inferred land cover change

(Fig. 7). This suggests that runoff- or snowmelt-generated flood frequencies at Nar Lake were controlled neither by the mean climate state nor by catchment land use. Variations in clastic layer thickness show a very different trend from frequency with a notable peak (i.e., thick turbidites) between 1000 and 700 cal BP (950-1250 CE), preceded and followed by phases when the clastic layers were much thinner and therefore unlikely to be true turbidites (Fig. 6). However, the clearest pattern emerges when frequency and magnitude are combined to calculate trends in total thickness of clastic sediment deposited on the lake bed (Figs. 6 and 7). When compared to $\delta^{18}O$-inferred climate, no clear correlation is apparent during the last 2500 years. There are peaks in total sediment influx during periods of both dry (e.g., 2000 cal BP) and wet climates (e.g., 900 cal BP). Some, but not all, periods of enhanced clastic layer deposition correspond to transitions from drier to wetter hydroclimatic conditions.

By contrast, an obvious match is seen between most of the clastic sedimentation maxima and pollen-inferred changes in land cover, especially forested land (Fig. 7). The times of maximum clastic influx occurred when forest cover was low and agricultural land use intensity was high in the area around Nar Lake. Similarly, minimum clastic influx corresponds to periods when forest cover expanded, notably between 1300 and 1000 cal BP. In a comparable study of flood layers in laminated lake sediments from northern Iberia, Corella et al. (2016) inferred that major sediment-transporting flood events increased during times of dry climate. However, here too, the main period of increased erosion corresponded to a period of expansion of population and agricultural land use into upland regions, in this case in Medieval times (Rull and Vegas-Vilarubia, 2015).

The close historical relationship between land cover and clastic sediment flux at Nar Lake allows further conclusions to be drawn. First, while runoff-generated flood or snowmelt events were clearly required in order to detach and transport sediment from the eroding catchment headslopes, the amount of sediment generated was greatly amplified by intensified human land use. Prior to 1300 cal BP, pollen evidence implies the presence of olive groves and vineyards close to Nar Lake. After 1000 cal BP, the dominant regional land use was agropastoralism (England et al., 2008), and

734 grazing animals (sheep/goat) probably played a significant part in vegetation
735 removal and exposure of bare ground to rain-splash erosion at Nar. Second, while the
736 fan delta at the southern edge of the lake changed the style of clastic sedimentation
737 (i.e., by causing turbidite deposition), there is no evidence for a lagged response in the
738 lake sediment record to external forcing. Nor is the event sequence an autocyclical
739 one, with sediment buildup in the fan delta leading to criticality and delta-front
740 failure. Hence this sediment store does not appear to have significantly delayed
741 transfer of sediment from the catchment to the lake bed. Consequently, clastic layers
742 in the lake can be used as a direct indicator of catchment erosion. Third, these results
743 imply that the most or all of the badland terrain currently existing on the Nar
744 catchment upper slopes formed during the late Holocene as a result of human
745 activity, rather than being ancient and of natural origin. Because some of these
746 badlands were excavated to form cave dwellings during Byzantine periods (primarily
747 1000-850 cal BP), then badland initiation clearly had to precede this time, most likely
748 between 2300 and 1300 cal BP.
749
750 The link between human activity and catchment erosion at Nar extends beyond the
751 lake sediment record to include historically attested changes in the rural economy
752 (e.g., Izdebski, 2013). For example, phase 2 of increased erosion and sediment influx
753 after 1000 cal BP (950 CE) corresponds to a time when a number of Anatolian
754 aristocratic landlords began to invest in expanding their estates after years of warfare
755 and insecurity, as testified in Byzantine documentary sources (Haldon et al., 2014).
756 Similarly the termination of this phase at 1250-1300 CE coincides with the Mongol
757 devastation of the Anatolian countryside during the 1260s, which in turn led to the
758 demise of the regional Selçuk polity in 1299. Significantly, the transfer of political
759 power from Byzantine to Selçuk rule after the battle of Manzikert/Malazgirt in 1071
760 CE did not lead to any diminution of erosion in the Nar catchment, suggesting
761 minimal economic-demographic rupture at this time. The correspondence between
762 these and other historically attested societal changes and the Nar Lake erosion record
763 is remarkable and reinforces the important role that human impact has played for
764 this geomorphic system.
765
766

6. Conclusions

The age of Cappadocia's hoodoos cannot be determined from a single site located at the periphery of the main area of badland terrain. Evidently, most of Cappadocia's badlands must be ancient and/or natural in origin, similar to other Mediterranean badlands in regions such as Almeria in Spain and Kokkinopolis in Greece (Thornes, 1987). The sequence of river terraces along the middle reach of the Kızılırmak implies a supply of sediment eroded from Cappadocia throughout the Quaternary (Doğan, 2010, 2011). Equally, no major alluvial-colluvial fill of late Holocene age has been reported at this potential depocentre. Nonetheless, our study from Nar Lake suggests that Cappadocia's badland terrain has become more extensive during the late Holocene and that the primary cause of this extension has been anthropogenic, via deforestation, cultivation of cereals and tree crops, and livestock grazing. Climate change may have played a synergistic role in accelerating erosion, notably during wet-dry or dry-wet transitional phases, and perhaps especially during an initial precocious phase of Neolithic landscape instability. However, on its own, climate change cannot explain the pattern in sediment flux into Nar Lake during the last ~14 ka. Lithogenic element concentrations or ratios (e.g., Ti/Ca) have sometimes been used as a proxy for runoff and rainfall in Mediterranean sedimentary records (e.g., Ülgen et al., 2012; Heymann et al., 2013), but in Nar Lake their explanation relates at least as much to human-induced land cover change as to palaeoclimate. For example, erosion rates remained low during the major climatic and vegetation transition of the Late Glacial to early Holocene, as they did during most times of extreme climatic aridity during the Bronze Age. The low rate of sediment flux during the Bronze Age is doubly surprising given regional archaeological evidence for demographic increase (Allcock and Roberts, 2014; Woodbridge et al., 2018, in press) and pollen and charcoal evidence of forest decline. Not all periods of regional demographic increase may have affected the immediate vicinity of Nar Lake, whose erosion history represents a signal of local land use. However, a similar trend characterised small stream catchments draining into the lower Orontes River at the northern end of the Levant near Antioch/Antakya (Casana, 2008). Here too, the major increase in sediment yield occurred with land use intensification during Classical rather than Bronze or Iron Age times. More widely across the Mediterranean, economic

intensification by complex societies during the second and third millennia BP led to major landscape changes and increased soil degradation (Walsh et al., in review).

During the last 2600 years, the varved nature of Nar Lake sediments has allowed an unusually detailed and well-dated record of clastic event pulses. Because of the existence of an alluvial fan delta on the lake edge, the most important of these depositional events were as turbidites rather than normal flood layers. Even so, pollen data show clearly that catchment erosion increased when there was more intense human land use (arable and grazing), notably during Classical, Medieval, and modern times. Similarly, erosion decreased when forest cover expanded, for example, between 1300 and 1000 cal BP. The evidence for landscape recovery at this and other times of reduced human pressure shows that even actively eroding badland terrain can heal itself if the *environmental footprint* of humans is reduced and sustained for sufficient time. The sedimentary record indicates that the current phase of accelerated erosion at Nar only started in ~1920 and that it was preceded by more than four centuries when erosion rates were substantially lower and apparently more sustainable. While not the natural baseline that existed during the early Holocene, the Ottoman period of moderate-intensity agropastoral land use could offer a realistic potential target state for geomorphological landscape restoration at this site. The Nar Lake catchment record thus appears to offer a historical geomorphological example of a scenario described by Butzer (1974, p. 73) showing how, 'with careful cultivation or pasturing of limited numbers of suitable livestock, soil erosion can be kept to an acceptable minimum'.

Acknowledgements

The fieldwork for this project was supported by funding from the British Institute in Ankara, the National Geographic Committee for Research and Exploration and from Plymouth University. We thank the Turkish Ministry of Environment and Forests for field research permission. Itrax measurement were carried out as part of a University of Plymouth PhD studentship to SA. Thin section analysis was carried out as part of a NERC ENVISION DTP funded PhD studentship to NP at Nottingham University. Isotope work was funded by NIGFSC grants IP/1198/1110 and IP/1237/0511 and by

NERC PhD studentship NE/I528477/1. We are also pleased to acknowledge the assistance of Jonathan Dean, Ann England, Melanie Leng, Jessie Woodbridge, Fabien Arnaud, Emmanuel Malet, Gwyn Jones, Ryan Smith, Andy Moss, Charu Sharma, Henry Lamb, Achim Brauer, Sarah Metcalfe, Mike Marshall, and two anonymous referees whose constructive critical comments substantially improved the paper.

References

Allcock, S.L., 2013. Living with a Changing Landscape: Holocene Climate Variability and Socio-evolutionary Trajectories, Central Turkey (Unpublished Ph.D. thesis), Plymouth University.

Allcock, S.L., 2017. Long-term socio-environmental dynamics and adaptive cycles in Cappadocia, Turkey during the Holocene. Quaternary International 446, 66-82.

Allcock, S.L., Roberts, N., 2014. Changes in regional settlement patterns in Cappadocia (central Turkey) since the Neolithic: a combined site survey perspective. Anatolian Studies 64, 33-58.

Ayala, G., Wainwright, J., Walker, J., Hodara, R., Lloyd, J.M., Leng, M., Doherty, C., 2017. Palaeoenvironmental reconstruction of the alluvial landscape of Neolithic Çatalhöyük, central southern Turkey: The implications for early agriculture and responses to environmental change. Journal of Archaeological Science 87, 30-43.

Balcı, S., 2010. Obsidian source-technology-settlement relations: Aşikli höyük (Central Anatolia) case. In: Matthiae, P., Pinnock, F., Nigro, L., Marchett. N. (Eds.) Proceedings of the 6th International Congress on the Archaeology of the Ancient Near East, Rome, Harrassowitz Verlag, Wiesbaden, pp.295-304.

Barnett, H., 2016. Source to sink sediment linkages in Nar lake Cappadocia. (Unpublished BSc dissertation, Physical Geography and Geology), Plymouth University.

Biernacki, C., Celeux, A., Govaert, G., Langrognet, F., 2006. Model-Based Cluster and Discriminant Analysis with the MIXMOD Software, Computational Statistics and Data Analysis, 51/52, 587-600.

Blass, A., Anselmetti, F.S., Grosjean, M., 2005. The last 1300 years of environmental history recorded in the sediments of Lake Sils (Engadine, Switzerland). Eclogae. Geol. Helv. 98, 319–332.

Boës, X., Fagel, N., 2005. Impregnation method for detecting annual laminations in sediment cores: an overview. Sedimentary Geology 179, 185-194

Boyer, P., Roberts, N., Baird, D., 2006. Holocene environment and settlement on the Çarşamba alluvial fan, South Central Turkey: Integrating Geoarchaeology and Archaeological Field Survey. GeoArchaeology 21, 675-699.

Brown, A.G., Tooth, S., Bullard, J.E., Thomas, D.S., Chiverrell, R.C., Plater, A.J., Murton, J., Thorndycraft, V.R., Tarolli, P., Rose, J., Wainwright, J., 2017. The geomorphology of the Anthropocene: emergence, status and implications. Earth Surface Processes and Landforms 42, 71-90.

Butzer, K.W., 1974. Accelerated soil erosion: a problem of man-land relationships. In: Perspectives on environment, Association of American Geographers, Commission on College Geography, Publication no. 13, pp. 57-77.

Butzer, K.W., 2005. Environmental history in the Mediterranean world: cross-disciplinary investigation of cause-and-effect for degradation and soil erosion. Journal of Archaeological Science 32(12), 1773-1800.

Carter, T., 2011. A true gift of mother earth: the use and significance of obsidian at Çatalhöyük. Anatolian Studies 61, 1-19.

Casana, J., 2008. Mediterranean Valleys revisited: Linking soil erosion, land use and climate variability in the northern Levant. Geomorphology 101, 429-42.

Corella, J.P., Valero-Garcés, B.L., Vicente-Serrano, S.M., Brauer, A., Benito, G., 2016. Three millennia of heavy rainfalls in Western Mediterranean: frequency, seasonality and atmospheric drivers. Scientific Reports, 6, p.38206.

Croudace, I.W., Rindby, A., Rothwell, R.G., 2006. ITRAX: description and evaluation of a new multi-function X-ray core scanner. Geological Society, London, Special Publications 267, 51–63.

Dean, J.R., Jones, M.D., Leng, M.J., Sloane, H.J., Swann, G.E.A., Metcalfe, S.E., Roberts, C.N., Woodbridge, J., Eastwood, W.J., Yiğitbaşıoğlu, H., 2013. Palaeo-seasonality of the last two millennia reconstructed from the oxygen isotope composition of diatom silica and carbonates from Nar Gölü, central Turkey. Quaternary Science Reviews 66, 35–44.

Dean, J.R., Eastwood, W.J., Roberts, N., Jones, M.D., Yiğitbaşıoğlu, H., Allcock, S.L., Woodbridge, J., Metcalfe, S.E., Leng, M.J., 2015a. Tracking the hydro-climatic signal from lake to sediment: a field study from central Turkey. J. Hydrol. 529, 608–621.

Dean, J.R., Jones, M.D., Leng, M.J., Noble, S.R., Metcalfe, S.E., Sloane, H.J, Sahya, D., Eastwood, W.J., Roberts, C.N., 2015b. Eastern Mediterranean hydroclimate over the late glacial and Holocene, reconstructed from the sediments of Nar lake, central Turkey, using stable isotopes and carbonate mineralogy. Quaternary Science Reviews 124, 162–174.

Doğan, U., 2010. Fluvial response to climate change during and after the Last Glacial Maximum in Central Anatolia, Turkey. Quaternary International 222 (1-2), 221-229.

929 Doğan, U., 2011. Climate-controlled river terrace formation in the Kızılırmak Valley,
930 Cappadocia section, Turkey: inferred from Ar–Ar dating of Quaternary basalts and
931 terraces stratigraphy. Geomorphology 126 (1-2), 66-81.
932
933 Dusar, B., Verstraeten, G., Notebaert, B., Bakker, J., 2011. Holocene environmental
934 change and its impact on sediment dynamics in the Eastern Mediterranean. Earth-
935 Science Reviews 108 (3), 137-157.
936
937 Dusar, B., Verstraeten, G., D'haen, K., Bakker, J., Kaptijn, E., Waelkens, M., 2012.
938 Sensitivity of the Eastern Mediterranean geomorphic system towards environmental
939 change during the Late Holocene: a chronological perspective. Journal of Quaternary
940 Science 27, 371-382.
941
942 Eastwood, W.J., Roberts, N., Lamb, H.F., Tibby, J.C., 1999. Holocene environmental
943 change in southwest Turkey: a palaeoecological record of lake and catchment-related
944 changes. Quaternary Science Reviews 18, 671-696.
945
946 England, A., Eastwood, W.J., Roberts, C.N., Turner, R., Haldon, J.F., 2008. Historical
947 landscape change in Cappadocia (central Turkey): a palaeoecological investigation of
948 annually-laminated sediments from Nar lake. The Holocene 18, 1229-1245.
949
950 Francus, P., Keimig, F., Besonen, M., 2002. An algorithm to aid varve counting and
951 measurement from thin-sections. Journal of Paleolimnology 28, 283-286
952
953 Gevrek, A.I., Kazancı, N., 2000. A Pleistocene, pyroclastic-poor maar from central
954 Anatolia, Turkey: influence of a local fault on a phreatomagmatic eruption. J. Volcanol.
955 Geotherm. Res. 95, 309–317.
956
957 Gilli, A., Anselmetti, F.S., Glur, L., Wirth, S.B., 2013. Lake sediments as archives of
958 recurrence rates and intensities of past flood events. In: Schneuwly- Bollschweiler, M.,
959 Stoffel, M., Rudolf-Miklau, F. (Eds.), Dating Torrential Processes on Fans and Cones –
960 Methods and Their Application for Hazard and Risk Assessment. Advances in Global
961 Change Research, 47. Springer Netherlands, pp. 225-242.

Grove, A.T., Rackham, O., 2001. The Nature of Mediterranean Europe: an Ecological History. Yale University Press, New Haven.

Haldon J., Izdebski A., Roberts N., Fleitmann D., McCormick M., Cassis M., Doonan O.P., Eastwood W.J., Elton H., Ladstätter S., Manning S., Newhard J., Nichol K., Telelis I.G., Xoplaki E., 2014. The climate and environment of Byzantine Anatolia: integrating science, history and archaeology. Journal of Interdisciplinary History 45, 113-161.

Hennekam, R., de Lange, G., 2012. X-ray fluorescence core scanning of wet marine sediments: methods to improve quality and reproducibility of high-resolution paleoenvironmental records. Limnology and Oceanography: Methods 10, 991-1003.

Heymann, C., Nelle, C., Dörfler, W., Zagana, H., Nowaczyk, N., Jibin Xue, Unkel, I., 2013. Late Glacial to mid-Holocene palaeoclimate development of Southern Greece inferred from the sediment sequence of Lake Stymphalia (NE-Peloponnese). Quaternary International 302, 42-60.

Hodder, I., 2014. Çatalhöyük: the leopard changes its spots. A summary of recent work. Anatolian Studies 64, 1-22.

Izdebski, A., 2013. A rural economy in transition: Asia Minor from Late Antiquity into the early Middle Ages. Journal of Juristic Papyrology supplement 18. Warsaw: Raphael Taubenschlag Foundation.

Jones, M.D., Leng, M.J., Roberts, N., Türkeş, M., Moyeed, R., 2005. A coupled calibration and modelling approach to the understanding of dry-land lake oxygen isotope records. Journal of Paleolimnology 34, 391-411. DOI 10.1007/s10933-005-6743-0

Jones, M.D., Roberts, N., Leng, M.J., Türkeş, M., 2006. A high-resolution late Holocene lake isotope record from Turkey and links to North Atlantic and monsoon climate. Geology 34 (5), 361-364. DOI: 10.1130/G22407.1

995 Juschus, O., Melles, M. Gebhardt, A.C., Niessen, F., 2009. Late Quaternary mass
996 movement events in Lake El'gygytgyn, North-eastern Siberia. Sedimentology 56,
997 2155-2174.
998
999 Kayacan, N., Özbaşaran, M., 2007. The Choice of Obsidian and its use at Musular,
1000 Central Anatolia. In: Astruc, L., Binder, D., Briois, F. (Eds.) Systèmes techniques et
1001 communautés du Néolithique précéramique au Proche-Orient. Éditions APDCA,
1002 Antibes, pp. 229-233.
1003
1004 Kylander, M.E., Ample, L., Wohlfarth, B., Veres, D., 2011. High-resolution X-ray
1005 fluorescence scanning analysis of Les Echets (France) sedimentary sequence: new
1006 insights from chemical proxies. Journal of Quaternary Science 26 (1), 109-117.
1007
1008 Macklin, M.G., Woodward, J.C., 2009. River systems and environmental change. In:
1009 Woodward, J. (Ed.) The Physical Geography of the Mediterranean. Oxford University
1010 Press, Oxford, pp. 319-352.
1011
1012 Mangili, C., Brauer, A., Moscariello, A., Naumann, R., 2005. Microfacies of detrital event
1013 layers deposited in Quaternary varved lake sediments of the Piànico-Sèllere Basin
1014 (northern Italy). Sedimentology 52, 927-943
1015
1016 Marsh, B., Kealhofer, L. 2014. Scales of impact: settlement history and landscape
1017 change in the Gordion region, central Anatolia. The Holocene 24, 689-701.
1018
1019 Marsh, G.P., 1864. Man and Nature (or Physical Geography as modified by human
1020 action).
1021
1022 Mouralis D, Pastre J-F, Kuzucuoğlu C, Türkecan A, Atıcı Y, Slimak L, Guillou H, Kunesch
1023 S., 2002. Les complexes volcaniques Rhyolithiques quaternaires d'Anatolie centrale
1024 (Göllü Dag et Acigöl, Turquie): Genèse, instabilité, contraintes environnementales.
1025 Quaternaire 13, 219-228
1026

Mulder, T., Syvitski, J.P.M., Migeon, S., Faugeres, J.C., Savoye, B., 2003. Marine hyperpycnal flows: Initiation, behaviour and related deposits. A review. Marine and Petroleum Geology 20, 861-882.

Nichols, G., 2009. Sedimentology and Stratigraphy. 2nd edition. Wiley: West Sussex.

Ojala, A.E.K., Francus, P., Zolitschka, B., Besonen, M., Lamoureux, S.F., 2012. Characteristics of sedimentary varve chronologies – a review. Quaternary Science Reviews 43, 45-60.

Osleger, D.A., Heyvaeart, A.C., Stoner, J.S., Verosub, K.L., 2009. Lacustrine turbidites as indicators of Holocene storminess and climate: Lake Tahoe, California and Nevada. Journal of Paleolimnology 42, 103–122.

Ousterhout, R., 1999. The Acıözü Churches near Celtek in Western Cappadocia. Cah.Arch. 47, 67-76.

Ousterhout, R., 2005. A Byzantine Settlement in Cappadocia, Dumbarton Oaks Studies 42, Washington, D.C.

Primmer, N., 2018. Reconstructing high resolution environmental change from carbonate-rich lakes in Turkey and Mexico using varve microfacies analysis. (Unpublished Ph.D. thesis), University of Nottingham, UK

Roberts, N. 2018. Re-visiting the Beyşehir Occupation phase: land-cover change and the rural economy in the eastern Mediterranean during the first millennium AD. In: Mulryan, M., Izdebski, A. (Eds.) Late Antique Archaeology 11, 53–68.

Roberts, N., Allcock, S.L., Arnaud, F., Dean, J.R., Eastwood, W.J., Jones, M.D., Leng, M.J., Metcalfe, S.E., Malet, E., Woodbridge, J., Yiğitbaşıoğlu, H., 2016. A tale of two lakes: a multi-proxy comparison of Late Glacial and Holocene environmental change in Cappadocia, Turkey. Journal of Quaternary Science 31(4), 348–362.

Roffet-Salque, M., Marciniak, A., Valdes, P.J., Pawłowska, K., Pyzel, J., Czerniak, L., Krüger, M., Roberts, N., Pitter, S., Evershed, R.P., 2018. Evidence for impact of the 8.2 kyr BP event on Near Eastern Neolithic farmers from multi-proxy records and climate modelling. Evidence for impact of the 8.2 kyr BP event on Near Eastern Neolithic farmers from multi-proxy records and climate modelling. Proceedings of the National Academy of Sciences 115(35), 8705-8709. doi/10.1073/pnas.1803607115

Rothwell, R.G., Rack, F.R., 2006. New techniques in sediment core analysis: an introduction. In: Rothwell RG, Rack FR (Eds). New Techniques in Sediment Core Analysis, Geological Society: London; pp. 1–29.

Rull, V., Vegas-Vilarrúbia, T., 2015. Crops and weeds from the Estany de Montcortès catchment, central Pyrenees, during the last millennium: a comparison of palynological and historical records. Vegetation History and Archaeobotany 24, 699-710

Sauerbrey, M.A., Juschus, O., Gebhardt, A.C., Wenrich, V., Nowaczyk, N.R., Melles, M., 2013. Mass movement deposits in the 3.6Ma sediment record of Lake El'gygytgyn, Far East Russian Arctic. Clim. Past. 9, 1949–1967.

Schmitt, A.K., Danišík, M., Aydar, E., Şen, E., Ulusoy, I., Lovera, O.M., 2014. Identifying the volcanic eruption depicted in a Neolithic painting at Çatalhöyük, Central Anatolia, Turkey. PLoS ONE 9(1), e84711.

Sherlock, R.L., 1922. Man as a Geological Agent: an Account of his Action on Inanimate Nature. H.F. & G. Witherby.

Smith, R., 2010. A Geophysical Survey of Nar Gölü, Cappadocia, Turkey. (unpublished MSc dissertation), University of Plymouth

Stokes, M., Mather, A.E., Harvey, A.M., 2002. Quantification of river capture induced base-level changes and landscape development, Sorbas Basin, SE Spain. In: Jones, S.J.,

Frostick, L.E. (Eds) Sediment Flux to Basins: Causes, Controls and Consequences. Geological Society, London Special Publication, 191, pp.23-35.

Strasser, M., Anselmetti, F.S., 2008. Mass-movement event stratigraphy in Lake Zurich: A record of varying seismic and environmental impacts. Beiträge zur Geologie der Schweiz, Geotechnische Serie 95, 23–41.

Sturm, M., Matter, A., 1978. Turbidites and Varves in Lake Brienz (Switzerland): Deposition of Clastic Detritus by Density Currents. In: Matter, A., Tucker, M.E. (Eds.) Modern and Ancient Lake Sediments, Blackwell Publishing Ltd., Oxford, pp.147-168.

Swierczynski, T., Lauterbach, S., Dulski, P., Delgado, J., Merz, B., Brauer, A., 2013. Mid- to late Holocene flood frequency changes in the northeastern Alps as recorded in varved sediments of Lake Mondsee (Upper Austria). Quaternary Science Reviews 80, 78-90.

Thierry, N., 2002. La Cappadoce de l'antiquité au Moyen Âge. Brepols.

Thornes, J.B., 1987. The palaeo-ecology of erosion, In: Wagstaff, J.M. (Ed.) Landscape and Culture. Basil Blackwell, Oxford, pp. 37-55.

Ülgen, U.B., Franz, S.O., Biltekin, D., Çagatay, M.N., Roeser, P.A. Doner, L., Thein, J., 2012. Climatic and environmental evolution of Lake Iznik (NW Turkey) over the last ~4700 years. Quaternary International 274, 88-101.

van Andel, T.H., Zangger, E., Demitrack, A., 1990. Land use and soil erosion in prehistoric and historical Greece. Journal of Field Archaeology 17, 379-396.

Vannière, B., Colombaroli, D., Chapron, E., Leroux, A., Tinner, W., Magny, M., 2008. Climate versus human-driven fire regimes in Mediterranean landscapes: the Holocene record of Lago dell'Accesa (Tuscany, Italy). Quaternary Science Reviews 27, 1181-1196.

Vannière B., Magny M., Joannin S., Simonneau A., Wirth S. B., Hamann Y., Chapron E., Gilli A., Desmet M., Anselmetti F. S., 2013. Orbital changes, variation in solar activity and increased anthropogenic activities: controls on the Holocene flood frequency in the Lake Ledro area, Northern Italy. Clim. Past 9, 1193-1209.

Vita-Finzi, C., 1969. The Mediterranean valleys. Cambridge: Cambridge University Press.

Wagstaff, J.M., 1981. Buried assumptions: some problems in the interpretation of the 'Younger Fill' raised by recent data from Greece. Journal of Archaeological Science 8, 247-64.

Walsh, K., Berger, J-F., Roberts, N., Vannière, B., Ghilardi, M., Brown, A.G., Woodbridge, J., Lespez, L., Estrany, J., Glais, A., Palmisano, A., Finné, M., Verstraeten, G., in review. Holocene demographic fluctuations, climate and erosion in the Mediterranean: a meta data-analysis. The Holocene

Woodbridge, J., Roberts, N., 2010. Linking neo and palaeolimnology: a case study using crater lake diatoms from central Turkey. Journal of Paleolimnology 44, 855-871. DOI 10.1007/s10933-010-9458-9

Woodbridge, J., Roberts, N., Palmisano, A., Bevan, A., Shennan, S., Fyfe, R., Eastwood, W.J., Izdebski, A., Çakırlar, C., Woldring, H., Broothaerts, N., Kaniewski, D., Finné, M., Labuhn, I., 2018, in press. Pollen-inferred regional vegetation patterns and demographic change in Southern Anatolia through the Holocene. The Holocene

Zanchetta, G., Sulpizio, R., Roberts, N., Cioni, R., Eastwood, W.J., Siani, G., Caron, B., Paterne, M., Santacroce, R., 2011. Tephrostratigraphy, chronology and climatic events of the Mediterranean basin during the Holocene: an overview. The Holocene 21, 33-52.